Reactions of Tertiary Phosphines, Phosphites, and Arsines with $[Ru(\eta^5\text{-}C_5H_5)(\eta^4\text{-}C_5H_4O)]^+$ Derivatives: X-ray Structures of $[Ru(\eta^5\text{-}C_5H_4PCy_3)(\eta^5\text{-}C_5H_4OH)]^+$, $[Ru(\eta^5\text{-}C_5H_5)(\eta^4\text{-}C_5H_4O)(P(OPh)_3)]^+$, and $[Ru(\eta^5\text{-}C_5H_5)(\eta^4\text{-}C_5H_3O\text{-}2\text{-}PPh_3)(MeCN)]^{2+}$

Karl Kirchner,*[1a] Kurt Mereiter,[1b] Roland Schmid,[1a] and Henry Taube[2]

Institute of Inorganic Chemistry and Institute of Mineralogy, Crystallography, and Structural Chemistry, Technical University of Vienna, Getreidemarkt 9, A-1060-Vienna, Austria, and Department of Chemistry, Stanford University, Stanford, California 94305

Received May 7, 1993[⊛]

Treatment of $[Ru(\eta^5\text{-}C_5H_5)(\eta^4\text{-}C_5H_4O)]_2(PF_6)_2$ (**1**) with PR_3 (R = Me, Cy, Ph) and $AsMe_3$ results in the formation of 1,1′-disubstituted ruthenocenes of types $[Ru(\eta^5\text{-}C_5H_4PR_3)(\eta^5\text{-}C_5H_4OH)]PF_6$ and $[Ru(\eta^5\text{-}C_5H_4AsMe_3)(\eta^5\text{-}C_5H_4OH)]PF_6$, respectively, in 50–60% yield. The crystal structure of $[Ru(\eta^5\text{-}C_5H_4PCy_3)(\eta^5\text{-}C_5H_4OH)]PF_6$ (**7**) has been determined by X-ray diffraction techniques. **7** crystallizes in the space group $P2_1/n$, with a = 16.207(3) Å, b = 15.680(3) Å, c = 11.245(2) Å, β = 92.24(1)°, V = 2855.5(9) Å^3, and Z = 4. The structure was refined to R = 0.034 and R_w = 0.038. $[Ru(\eta^5\text{-}C_5H_5)(\eta^4\text{-}C_5H_4O)(CH_3CN)]PF_6$ (**2**) reacts with PR_3 (R = Me, Cy) to give the same products as does **1**, whereas with PPh_3 a different pathway is observed, giving $[Ru(\eta^5\text{-}C_5H_5)(\eta^5\text{-}C_5H_3OH\text{-}2\text{-}PPh_3)]PF_6$ (**9**) in 60% yield. On treatment of **2** with $AsMe_3$, $[Ru(\eta^5\text{-}C_5H_5)(\eta^4\text{-}C_5H_4O)(AsMe_3)]PF_6$ (**11**) is obtained as the major product together with a small amount of $[Ru(\eta^5\text{-}C_5H_5)(\eta^5\text{-}C_5H_3OH\text{-}2\text{-}AsMe_3)]PF_6$ (**12**). Complexes **1** and **2** react readily with $P(OPh)_3$ to form $[Ru(\eta^5\text{-}C_5H_5)(\eta^4\text{-}C_5H_4O)(P(OPh)_3)]PF_6$ (**13**). A single-crystal structural study has been carried out for this complex. The space group is $P\bar{1}$, with a = 9.995(2) Å, b = 10.412(2) Å, c = 14.327(2) Å, α = 104.88(1)°, β = 103.83(1)°, γ = 92.51(1)°, V = 1390.4(5) Å^3, and Z = 2. The structure was refined to R = 0.033 and R_w = 0.038. Reactions of **1** with $P(OMe)_3$ result in several products which have not yet been identified. Oxidation of $[Ru(\eta^5\text{-}C_5H_4PPh_3)(\eta^5\text{-}C_5H_4OH)]PF_6$ (**8**) by Br_2 in nitromethane as a solvent yields $[Ru(\eta^5\text{-}C_5H_4PPh_3)(\eta^4\text{-}C_5H_4O)\,Br]PF_6$ (**15**) in quantitative yield. Though **15** appears to be stable in solution it could not be isolated as a solid. I_2 and Ag^+ did not react with **8**. Species **9** undergoes facile oxidation reactions with Br_2, I_2, and Ag^+ (in CH_3CN as solvent) to give the novel complexes $[Ru(\eta^5\text{-}C_5H_5)(\eta^4\text{-}C_5H_3O\text{-}2\text{-}PPh_3)Br]PF_6$ (**16**), $[Ru(\eta^5\text{-}C_5H_5)(\eta^4\text{-}C_5H_3O\text{-}2\text{-}PPh_3)I]PF_6$ (**17**), and $[Ru(\eta^5\text{-}C_5H_5)(\eta^4\text{-}C_5H_3O\text{-}2\text{-}PPh_3)(CH_3CN)](PF_6)_2$ (**18**). $[Fe(\eta^5\text{-}C_5H_5)_2]PF_6$ does not react with **9**. Compound **18** has been found to crystallize in space group *Pbca*, with a = 20.835(4) Å, b = 19.457(4) Å, c = 16.096(3) Å, V = 6525(2) Å^3, and Z = 8. The discrepancy factors R and R_w are 0.051 and 0.055, respectively. The reactivity pattern of **1** and **2** toward nucleophiles is discussed in terms of a strong resonance interaction between the metal and the ketonic group, leading to Ru(II) and Ru(IV) limiting structures.

Introduction

Cyclopentadienone (C_5H_4O) in the free state is a highly unstable molecule subject to rapid dimerization but it can be stabilized upon coordination to transition metals. Accessibility to such complexes, however, is limited since, owing to the instability of C_5H_4O, its complexes are arrived at by carrying out reactions on suitable precursor complexes. It is, thus, understandable that not many complexes of the simple ligand are described in the literature. Examples include the neutral species $Fe(\eta^4\text{-}C_5H_4O)(CO)_3$,[3] and $Ru(\eta^5\text{-}C_5H_5)(\eta^4\text{-}C_5H_4O)Br$,[4] and the cationic complex $[Mo(CO)_2(\eta^5\text{-}C_5H_5)(\eta^4\text{-}C_5H_4O)]PF_6$.[5]

We recently reported the syntheses of a series of complexes containing unsubstituted cyclopentadienone, among them $[Ru(\eta^5\text{-}C_5H_5)(\eta^4\text{-}C_5H_4O)]_2(PF_6)_2$, **1**, and $[Ru(\eta^5\text{-}C_5H_5)(\eta^4\text{-}C_5H_4O)(CH_3CN)]PF_6$, **2**, and gave a preliminary account of their reactions with nucleophiles.[6,7] With the nucleophiles Cl^-, Br^-, I^-, pyridine, isocyanides, thioethers, and several others, simple ligand substitution on the metal center takes place, yielding a range of new complexes with a variety of coligands attached to the $[Ru(\eta^5\text{-}C_5H_5)(\eta^4\text{-}C_5H_4O)]^+$ moiety.[7] Other nucleophiles, among them PR_3, SR^- (R = Me, Ph) and CN^-, reacted with **1** by substituting on the $C_5H_5^-$ ring, while with **2** in some cases substitution took place also at the C_5H_4O ligand,[6] both kinds of reaction being unprecedented. The η^4-cyclopentadienone ligand was in each case converted into η^5-hydroxycyclopentadienyl.

It is generally accepted that activation of the electron-rich ligand $C_5H_5^-$ toward nucleophilic substitution is difficult.[8] Thus, our observations are of intrinsic interest and may also be useful for the development of synthetic organic methodology. The chemoselectivity of these reactions is remarkable, especially bearing in mind that coordinated η^4-dienes are among the most reactive substrates toward nucleophiles. The X-ray structures of **1**, **2**, $Ru(\eta^5\text{-}C_5H_5)(\eta^4\text{-}C_5H_4O)Br$ and $Fe(\eta^4\text{-}C_5H_4O)(CO)_3$ reveal an η^4-binding mode of C_5H_4O where the ketonic group is out-of-plane of the butadiene system and bent away from the metal.[4,7,9] Therefore, regioselective attack in α position to the ketone functional group of cyclopentadienone rather than at the C_5H_5 ring might be expected.[8] In fact, it has been shown recently that the cationic complex $[Mo(CO)_2(\eta^5\text{-}C_5H_5)(\eta^4\text{-}C_5H_4O)]^+$ reacts with various nucleophiles to give exclusively neutral η^3-cyclo-

⊛ Abstract published in *Advance ACS Abstracts,* October 15, 1993.

(1) (a) Institute of Inorganic Chemistry, Technical University of Vienna. (b) Institute of Mineralogy, Crystallography, and Structural Chemistry, Technical University of Vienna.
(2) Stanford University.
(3) (a) Reppe, W.; Vetter, H. *Justus Liebigs Ann. Chem.* **1953**, *582*, 133. (b) Green, M. L. H.; Pratt, L.; Wilkinson, G. *J. Chem. Soc.* **1960**, 989.
(4) Smith, T. P.; Kwan, K. S.; Taube, H.; Bino, A.; Cohen, S. *Inorg. Chem.* **1984**, *23*, 1943.
(5) Liebeskind, L. S.; Bombrun, A. *J. Am. Chem. Soc.* **1991**, *113*, 8736.
(6) Kirchner, K.; Taube, H. *J. Am. Chem. Soc.* **1991**, *113*, 7039.
(7) Kirchner, K.; Taube, H.; Scott, B.; Willett, R. D. *Inorg. Chem.* **1993**, *32*, 1430.
(8) Davies, S. G.; Green, M. L. H.; Mingos, D. M. P. *Tetrahedron* **1978**, *34*, 3047 (see especially p 3055).
(9) Hoffman, K.; Weiss, E. *J. Organomet. Chem.* **1977**, *128*, 237.

0020-1669/93/1332-5553$04.00/0

pentenoyl complexes in line with the anticipated reactivity pattern (reaction 1).[5] Regioselective substitution at the carbon adjacent

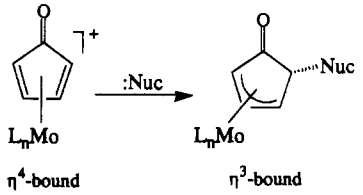

(1)

to the ketone was also observed in a few cases, but the reaction proceeds via a redox pathway yielding complexes with monosubstituted η^5-hydroxycyclopentadienyl (reaction 2).[6]

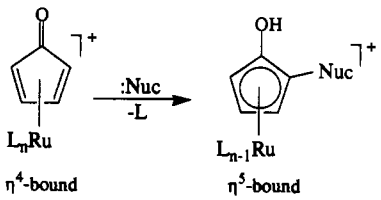

(2)

The unusual reactivity of complexes **1** and **2** toward nucleophiles has motivated the present study undertaken to extend the chemistry of $[Ru(\eta^5\text{-}C_5H_5)(\eta^4\text{-}C_5H_4O)]^+$ complexes. Here we describe the reactivity of **1** and **2** toward some tertiary phosphines, phosphites, and arsines. We report the X-ray crystal structures of three representative complexes resulting from the various reaction pathways and describe some reactions of such products.

Experimental Section

General Information. Manipulations were performed under an inert atmosphere of purified nitrogen by using standard Schlenk techniques and/or a glovebox unless otherwise noted. All chemicals were standard reagent grade and used without further purification. The solvents were purified according to standard procedures.[10] In order to remove propionitrile, nitromethane was purified by crystallization[11] followed by fractional distillation. The deuterated solvents were purchased from Aldrich and dried over 4-Å molecular sieves. IR spectra were obtained on IBM 98 and Mattson RS1 FTIR spectrometers. ^1H and ^{13}C NMR spectra were recorded on Nicolet NT-300 WB, Varian XL-400, Varian Gemini 200, and Bruker AC 250 spectrometers and were referenced to $SiMe_4$. ^{31}P NMR spectra were recorded on a Bruker AC 250 spectrometer and referenced to PPh_3. Microanalyses were conducted by Desert Analytics Laboratories, Tucson, AZ, and Microanalytical Laboratories, University of Vienna, Vienna, Austria. The syntheses of the starting materials $[Ru(\eta^5\text{-}C_5H_5)(\eta^4\text{-}C_5H_4O)]_2(PF_6)_2$ (**1**),[6] $[Ru(\eta^5\text{-}C_5H_5)(\eta^4\text{-}C_5H_4O)(CH_3CN)]PF_6$ (**2**),[6] $[Ru(\eta^5\text{-}C_5H_5)(\eta^4\text{-}C_5H_4O)(S(C_2H_5)_2)]PF_6$ (**3**),[7] $[Ru(\eta^5\text{-}C_5H_5)(\eta^4\text{-}C_5H_4O)(NC_5H_5)]PF_6$ (**4**),[7] and $Ru(\eta^5\text{-}C_5H_5)(\eta^4\text{-}C_5H_4O)Br$ (**5**),[4] followed procedures as referenced.

Reactions of 1 and 2 with Tertiary Phosphines, Phosphites, and Arsines. $[Ru(\eta^5\text{-}C_5H_4PMe_3)(\eta^5\text{-}C_5H_4OH)]PF_6$ (6). (a) A solution of **1** (200 mg, 0.25 mmol) in nitromethane (5 mL) was treated with trimethylphosphine, PMe_3, (85 μL, 0.52 mmol). The solution turned yellow instantaneously and upon treatment with diethyl ether a pale yellow precipitate was formed which was collected on a glass frit, washed with diethyl ether, and air dried. Yield: 131 mg (55%). Anal. Calcd for $C_{13}H_{18}OP_2F_6Ru$: C, 33.42; H, 3.88; P, 13.26; F, 22.39. Found: C, 34.10; H, 3.85; P, 12.34; F, 23.82. ^1H NMR (δ, acetone-d_6, 20°C): 5.06 (m, 2H), 5.00 (m, 2H), 4.85 (t, 2H), 4.42 (t, 2H), 3.79 (b, 1H), 2.04 (d, 9H, J_{HP} = 14.7 Hz). $^{13}C\{^1H\}$ NMR (δ, acetone-d_6, 20°C): 128.0 (C–O), 75.8 (d, J_{CP} = 10.7 Hz), 74.1 (d, J_{CP} = 14.5 Hz), 67.6, 66.4 (d, J_{CP} = 99.9 Hz), 63.2, 10.5 (d, J_{CP} = 59.3 Hz). (b) Compound **6** was also prepared in the same manner as described above with **2** as starting material, yield 57%.

$[Ru(\eta^5\text{-}C_5H_4PCy_3)(\eta^5\text{-}C_5H_4OH)]PF_6$ (7). This complex was prepared analogously to **3** with either **1** or **2** and tricyclohexylphosphine, PCy_3, as starting material. Yield: 59%. Anal. Calcd for $C_{28}H_{42}OP_2F_6Ru$: C, 50.07; H, 6.30; P, 9.22. Found: C, 49.96; H, 6.86; P, 9.23. ^1H NMR (δ, acetonitrile-d_3, 20°C): 4.92 (m, 2H), 4.85 (m, 2H), 4.67 (t, 2H), 4.31 (t, 2H), 2.60–2.40 (m, 3H), 2.20–1.20 (m, 30H). $^{13}C\{^1H\}$ NMR (δ, acetonitrile-d_3, 20°C): 127.5 (C–O), 76.2 (d, J_{CP} = 8.5 Hz), 75.8 (d, J_{CP} = 9.8 Hz,), 59.7 (d, J_{CP} = 84.4 Hz), 68.8, 64.2, 31.7 (d, J_{CP} = 43.8 Hz), 27.7 (d, J_{CP} = 3.4 Hz), 26.9 (d, J_{CP} = 12.2 Hz), 26.1. IR (KBr): 1513 cm^{-1} (s, ν_{C-O}).

$[Ru(\eta^5\text{-}C_5H_4PPh_3)(\eta^5\text{-}C_5H_4OH)]PF_6$ (8). This compound was prepared analogously to **3** with **1** and triphenylphosphine, PPh_3 (3-mol excess), as starting material. Yield: 50%. Anal. Calcd for $C_{28}H_{24}OP_2F_6Ru$: C, 51.46; H, 3.70; P, 9.48; F, 17.44. Found: C, 51.92; H, 3.69; P, 9.55; F, 17.36. ^1H NMR (δ, acetonitrile-d_3, 20°C): 7.95–7.77 (m, 15H), 5.89 (s, 1H), 5.09 (m, 2H), 4.83 (m, 2H), 4.51 (t, 2H), 4.19 (t, 2H). $^{13}C\{^1H\}$ NMR (δ, acetone-d_6, 20°C): 136.6 (d, J_{CP} = 3.0 Hz), 135.4 (d, J_{CP} = 10.6 Hz), 131.6 (d, J_{CP} = 12.8 Hz), 129.0 (C–O), 122.1 (d, J_{CP} = 92.0 Hz), 78.2 (d, J_{CP} = 10.6 Hz), 77.6 (d, J_{CP} = 13.8 Hz), 69.6, 65.0, 64.7 (d, J_{CP} = 106.2 Hz). IR (KBr): 1520 cm^{-1} (s, ν_{C-O}).

$[Ru(\eta^5\text{-}C_5H_5)(\eta^5\text{-}C_5H_3OH\text{-}2\text{-}PPh_3)]PF_6$ (9). **2** (150 mg, 0.35 mmol) and PPh_3 (91 mg, 0.35 mmol) were dissolved in 5 mL of acetone and stirred at room temperature for 8 h. The solvent and the liberated CH_3CN were removed under vacuum, and the crude product was redissolved in 2 mL of acetone. Upon addition of ca. 50 mL of diethyl ether the solution turned cloudy and was kept at −20 °C overnight. During this time off-white crystals were formed which were collected on a glass-frit, washed with diethyl ether and dried under vacuum. Yield: 137 mg (60.4%). Anal. Calcd for $C_{28}H_{24}OP_2F_6Ru$: C, 51.46; H, 3.70; P, 9.48. Found: C, 51.67; H, 3.48; P, 9.41. ^1H NMR (δ, acetone-d_6, 20°C): 8.00–7.78 (m, 15H), 5.21 (m, 1H), 4.76 (m, 1H), 4.57 (s, 5H), 4.16 (m, 1H). $^{13}C\{^1H\}$ NMR (δ, acetonitrile-d_3, 20°C): 135.8 (d, J_{CP} = 3.6 Hz), 135.0 (d, J_{CP} = 10.9 Hz), 130.8 (d, J = 13.2 Hz), 129.4 (C–O, d, J_{CP} = 7.0 Hz), 121.4 (d, J_{CP} = 93.3 Hz), 74.5 (C_5H_5), 72.3 (d, J_{CP} = 13.2 Hz), 70.2 (d, J_{CP} = 10.8 Hz), 65.8 (d, J_{CP} = 9.0 Hz), 55.3 (d, J_{CP} = 104.5 Hz). IR (KBr): 1520 cm^{-1} (s, ν_{C-O}).

$[Ru(\eta^5\text{-}C_5H_4AsMe_3)(\eta^5\text{-}C_5H_4OH)]PF_6$ (10). This complex was synthesized analogously to **3** with **1** and trimethylarsine, $AsMe_3$ (1 equiv), as starting materials. Yield: 60%. Anal. Calcd for $C_{13}H_{18}OAsPF_6Ru$: C, 30.54; H, 3.55. Found: C, 30.26; H, 3.31. ^1H NMR (δ, nitromethane-d_3, 20°C): 5.30 (b, 1H), 5.01 (m, 2H), 4.98 (m, 2H), 4.84 (t, 2H), 4.43 (t, 2H), 2.08 (s, 9H). $^{13}C\{^1H\}$ NMR (δ, acetone-d_3, 20°C): 127.9 (C–O), 75.3, 74.0, 69.7 (C-As), 67.9, 63.6, 10.3 (Me).

$[Ru(\eta^5\text{-}C_5H_5)(\eta^4\text{-}C_5H_4O)(AsMe_3)]PF_6$ (11). **2** (150 mg, 0.35 mmol) was dissolved in acetone (2 mL) and was treated with $AsMe_3$ (74 μL, 0.69 mmol). The reaction mixture was stirred for 3 h at 50 °C. Bright yellow crystals were formed slowly and were collected on a glass frit, washed with diethyl ether, and air-dried. Yield: 101 mg (57%). Anal. Calcd for $C_{13}H_{18}OAsPF_6Ru$: C, 30.54; H, 3.55. Found: C, 30.45; H, 3.30. ^1H NMR (δ, nitromethane-d_3, 20°C): 6.14 (m, 2H), 5.53 (s, 5H), 4.26 (m, 2H), 1.78 (s, 9H). $^{13}C\{^1H\}$ NMR (δ, nitromethane-d_3, 20°C): 181.6 (C=O), 85.3 (C_5H_5), 82.5, 68.6, 12.8 (Me).

$[Ru(\eta^5\text{-}C_5H_5)(\eta^5\text{-}C_5H_3OH\text{-}2\text{-}AsMe_3)]PF_6$ (12). Because of difficulty in separating small amounts (≤5% total yield, determined by ^1H NMR spectroscopy with crude reaction mixture) of **12** formed during the synthesis of **11**, no attempts were made to isolate this complex. However, its structure was deduced from the ^1H NMR spectrum, which is similar to that of **9**. ^1H NMR (δ, acetone-d_6, 20°C): 4.94 (m, 1H), 4.76 (s, 5H), 4.67 (m, 1H), 4.57 (m, 1H), 2.24 (s, 9H).

$[Ru(\eta^5\text{-}C_5H_5)(\eta^4\text{-}C_5H_4O)(P(OPh)_3)]PF_6$ (13). A 300-mg (0.43-mmol) sample of **1** and triphenyl phosphite, $P(OPh)_3$, (1.32 g, 4.3 mmol) were dissolved in nitromethane (5 mL), and the mixture was stirred at 70 °C for 5 h. The volume of the solution was then reduced to about 1 mL. Upon treatment with diethyl ether a yellow precipitate was formed, which was collected on a glass frit, washed several times with diethyl ether, and air-dried. Yield: 495 mg (92%). Anal. Calcd for $C_{28}H_{24}O_4P_2F_6Ru$: C, 47.94; H, 3.45; P, 8.83. Found: C, 47.67; H, 3.52; P, 8.67. ^1H NMR (δ, acetonitrile-d_3, 20°C): 7.40–7.20 (m, 15H), 6.16 (m, 2H), 5.70 (s, 5H), 3.77 (m, 2H). $^{13}C\{^1H\}$ NMR (δ, nitromethane-d_3, 20 °C): 183.6 (C=O), 152.5 (d, J_{CP} = 9.5 Hz), 131.5, 127.3, 122.0 (d, J_{CP} = 5.3 Hz), 87.8 (C_5H_5), 84.5 (d, J_{CP} = 2.5 Hz), 71.2 (d, J_{CP} = 3.6 Hz).

Reaction of 1 with $P(OMe)_3$. **1** (200 mg, 0.26 mmol) was dissolved in nitromethane-d_3 (3 mL) and was treated with trimethyl phosphite, $P(OMe)_3$, (32 mg, 0.26 mmol). Within a few minutes the color changed from red to brown, and the reaction mixture was transferred into a NMR tube. A ^1H NMR spectrum was immediately recorded and showed quantitative consumption of **1**. Among several decomposition products, two 1,1′-disubstituted ruthenocenes were formed in a ratio of 1:2 according to the ^1H NMR spectrum (δ 4.94 (m, 2H), 4.87 (m, 2H), 4.70

(10) Perrin, D. D.; Armarego, W. L. F. *Purification of Laboratory Chemicals*, 3rd ed.; Pergamon: New York, 1988.
(11) Parrett, F. W.; Sun, M. S. *J. Chem. Educ.* **1977**, *54*, 448.

(t, 2H), 4.37(t, 2H); 5.14 (m, 2H), 5.11 (m, 2H), 4.68 (t, 2H), 4.49 (t, 2H)). None of these decomposition products could be isolated and identified.

Reaction of 8 with Propionyl Chloride. [Ru(η^5-$C_5H_4PPh_3$)(η^5-$C_5H_4OCOC_2H_5$)]PF_6 (14). A 100-mg (0.15-mmol) sample of **8** and 15.5 mg (0.15 mmol) of triethylamine were dissolved in 2 mL of nitromethane. Then 14.2 mg (0.15 mmol) propionyl chloride was added, and the solution was stirred for 1 h. Upon addition of 5 mL of diethyl ether a precipitate of triethylamine hydrochloride was formed, which was removed by filtration. After addition of an additional 20 mL of diethyl ether, an off-white precipitate was slowly formed. It was collected on a glass frit, washed with diethyl ether, and air-dried. Yield: 60 mg (54%). Anal. Calcd for $C_{31}H_{28}O_2P_2F_6Ru$: C, 52.47; H, 3.98; P, 8.73. Found: C, 52.55; H, 4.01; P, 8.88. ^{1}H NMR (δ, acetone-d_6, 20°C): 8.00–7.80 (m, 15H), 5.29 (m, 2H), 5.12 (m, 2H), 4.93 (t, 2H), 4.44 (t, 2H), 2.35 (q, 2H), 1.06 (t, 3H).

Reaction of 8 with Br_2. [Ru(η^5-$C_5H_4PPh_3$)(η^4-C_5H_4O)Br]PF_6 (15). A 5-mm NMR tube was charged with **8** (17 mg, 0.026 mmol) in CD_3NO_2 (0.5 mL) and was capped with a septum. Br_2 (ca 1.3 μL, 0.026 mmol) was added by syringe, and the sample was transferred to a NMR probe. A ^{1}H NMR spectrum was immediately recorded and showed essentially quantitative formation of **15**. In solution **15** was stable for several days; however, attempts to isolate this complex were unsuccessful. ^{1}H NMR (δ, nitromethane-d_3, 20°C): 8.10–7.70 (m, 15H), 6.32 (m, 2H), 6.25 (m, 2H), 5.77 (t, 2H), 5.07 (t, 2H). ^{13}C{^{1}H} NMR (δ, nitromethane-d_3, 20°C): 179.3 (C=O), 137.7 (d, J_{CP} = 3.4 Hz), 136.1 (d, J_{CP} = 11 Hz), 132.0 (d, J_{CP} = 13.4 Hz), 117.7 (d, J_{CP} = 92.6 Hz), 101.0, 90.3 (d, J_{CP} = 8.5 Hz), 85.7, 80.8 (d, J_{CP} = 97.0 Hz), 73.7.

Attempted Reactions of 8 with I_2, and Ag^+. These reactions were performed on a scale suitable for NMR experiments. **8** (20 mg, 0.030 mmol) was dissolved in 0.5 mL of CD_3NO_2 and treated with either I_2 (77 mg, 0.300 mM) or Ag^+ (77 mg, 0.030 mmol, as PF_6^- salt). The reaction mixtures were loaded into NMR tubes, and ^{1}H NMR spectra were recorded. After 3 days, no reaction had occurred and ≥97% of **8** remained.

Reactions of 9 with Br_2 and I_2. [Ru(η^5-C_5H_5)(η^4-C_5H_3O-2-PPh_3)-Br]PF_6 (16). **9** was prepared in situ as described above by the action of PPh_3 (303 mg, 1.16 mmol) on **2** (500 mg, 1.16 mmol) in acetone (5 mL) and was redissolved in nitromethane (2 mL). Br_2 (60 μL, 1.16 mmol) was added by syringe, and the mixture was stirred for 1 h at room temperature. Upon addition of diethyl ether a pink precipitate was immediately formed which was collected on a glass frit, washed with diethyl ether, and air-dried. The crude product was redissolved in nitromethane (2 mL), and solid materials were removed by filtration. Addition of diethyl ether resulted in the precipitation of **16** as a pink powder. Yield: 677 mg (79 %). Anal. Calcd for $C_{28}H_{23}OBrP_2F_6Ru$: C, 45.92; H, 3.16; Br, 10.91; P, 8.46. Found: C, 45.03; H, 2.92; Br, 11.98; P, 8.13. ^{1}H NMR (δ, nitromethane-d_3, 20°C): 7.95–7.70 (m, 15H), 6.49 (m, 1H), 5.96 (m, 1H), 5.39 (s, 5H), 4.75 (m, 1H). ^{13}C{^{1}H} NMR (δ, nitromethane-d_3, 20°C): 180.8 (C=0), 136.6 (d, J_{CP} = 3.0 Hz), 135.9 (d, J_{CP} = 10.9 Hz), 131.3 (d, J_{CP} = 12.9 Hz), 119.3 (d, J_{CP} = 91.5 Hz), 89.2 (C_5H_5), 87.1 (d, J_{CP} = 9.7 Hz), 83.6 (d, J_{CP} = 11.3 Hz), 81.9 (d, J_{CP} = 11.9 Hz), 61.9 (d, J_{CP} = 87.5 Hz). IR (KBr): 1690 cm^{-1} ($\nu_{C=O}$).

Attempted Reaction of 9 with [Fe(η^5-C_5H_5)$_2$]PF_6. **9** (100 mg, 0.15 mmol) dissolved in CH_3NO_2 (3 mL) was treated with [Fe(η^5-C_5H_5)$_2$]-PF_6 (101 mg, 0.30 mmol), and the blue reaction mixture was stirred for 2 days. Upon addition of "peroxidized" diethyl ether (100 mL), a color change from blue to orange was observed and an off-white precipitate was formed slowly, which was filtered, washed with diethyl ether, and air-dried. After being opened to the air for approximately 2 weeks, diethyl ether usually contains sufficient hydroperoxide for that reaction. Examination of the ^{1}H NMR spectrum showed that this product was identical with the starting material, and no evidence for the presence of an oxidized species was found.

[Ru(η^5-C_5H_5)(η^4-C_5H_3O-2-PPh_3)I]PF_6 (17). A 5-mm NMR tube was charged with **9** (15 mg, 0.023 mmol) in CD_3NO_2 (0.5 mL). I_2 (58 mg, 0.230 mmol) was added, and the sample was transferred to a NMR probe. A ^{1}H NMR spectrum was immediately recorded and showed that no reaction had occurred. However, prolonged reaction times (3 days) resulted in the quantitative formation of **17**. ^{1}H NMR (δ, nitromethane-d_3, 20°C): 7.90–7.60 (m, 15H), 6.31 (m, 1H), 5.83 (m, 1H), 5.40 (s, 5H), 4.73 (m, 1H). No attempts were made to isolate **17**.

Reaction of 9 with Ag^+. [Ru(η^5-C_5H_5)(η^4-C_5H_3O-2-PPh_3)(CH_3CN)]-(PF_6)$_2$ (18). (a) **9** (150 mg, 0.23 mmol) was dissolved in acetonitrile (5 mL) and treated with $AgPF_6$ (116 mg, 0.46 mmol) for 2 h. Solid materials were removed by filtration. The solution was set aside for crystallization by vapor diffusion with diethyl ether. Small orange-brown crystals together with pale-yellow crystals were obtained after 1 day. These two products were separated manually, resulting in 91 mg (47%) of the desired compound. The pale-yellow product, presumably a $AgPF_6$ solvent adduct, was very hygroscopic, and was not further characterized. Anal. Calcd for $C_{30}H_{26}NOP_3F_{12}Ru$: C, 42.97; H, 3.13; N, 1.67; P, 11.08. Found: C, 42.99; H, 3.15; N, 1.70; P, 11.01. ^{1}H NMR (δ, nitromethane-d_3, 20°C): 8.00–7.80 (m, 15H), 6.84 (m, 1H), 6.48 (m, 1H), 5.66 (s, 5H), 5.26 (m, 1H), 2.44 (s, 3H). ^{13}C{^{1}H} NMR (δ, nitromethane-d_3, 20°C): 180.5 (d, J_{CP} = 6.4 Hz, C=O), 137.2 (d, J_{CP} = 2.9 Hz), 135.8 (d, J_{CP} = 11.1 Hz), 131.8 (d, J_{CP} = 12.9 Hz), 124.9 (CN), 118.0 (d, J_{CP} = 92.3 Hz), 92.6 (d, J_{CP} = 9.5 Hz), 90.9 (C_5H_5), 88.8 (d, J_{CP} = 10.2 Hz), 83.8 (d, J_{CP} = 9.9 Hz), 66.9 (d, J_{CP} = 86.6 Hz), 5.6 (CH_3). IR (KBr): 2326, 2299 (m, ν_{CN}), 1703 cm^{-1} (s, $\nu_{C=O}$). (b) $AgPF_6$ (69 mg, 0.27 mmol) was added to a flask containing **16** (200 mg, 0.27 mmol) dissolved in acetonitrile (3 mL). After the reaction mixture was stirred for 1 h, AgBr was removed by filtration, and the crude product was precipitated with diethyl ether as an orange-brown solid. In order to remove AgBr completely the complex was redissolved in nitromethane (3 mL). Solid materials were removed by filtration, and analytically pure product was obtained upon precipitation with diethyl ether. Yield: 160 mg (70%). Crystals were grown by vapor diffusion with diethyl ether.

Reactions of [Ru(η^5-C_5H_5)(η^4-C_5H_4O)L]$^{n+}$ (L = SEt_2 (3), NC_5H_5 (4), Br^- (5)) with PPh_3. These reactions were performed on a scale suitable for NMR experiments. Typically, 20 mg of the respective complex and PPh_3 (1 equiv) were dissolved in CD_3NO_2 (0.5 mL). The solutions were transferred into a NMR tube, and the reactions were monitored by ^{1}H and ^{31}P NMR spectroscopy. An account of this preliminary investigation will be given in the Results section.

Crystallography. Crystal data and experimental details are given in Table I. X-ray data were collected on a Philips PW1100 four-circle diffractometer using graphite monochromated Mo Kα (λ = 0.710 69 Å) radiation, and the θ-2θ scan technique. Three representative reference reflections were measured every 120 min and used to correct for crystal decay (small in all cases) and system instability. Data reduction included corrections for background and Lorentz and polarization factors and in two cases also for absorption. The program SHELX76[12] was used for structure solution and refinement; the XTAL3.0 suite of programs[13] was used to produce molecular diagrams and tabular matter.

[Ru(η^5-$C_5H_4PCy_3$)(η^5-C_5H_4OH)]PF_6 (7). A yellowish crystal measuring approximately 0.28 × 0.30 × 0.44 mm was used for data collection. This crystal was a fragment of a larger contact twin similar in appearance to a gypsum dovetail twin. No absorption correction was applied. The structure was solved using the Patterson method, which revealed the

Table I. Crystallographic Data for **7**, **13**, and **18**

	7	13	18
formula	$RuC_{28}H_{42}F_6OP_2$	$RuC_{28}H_{24}F_6O_4P_2$	$RuC_{30}H_{26}F_{12}NOP_3$
fw	671.65	701.50	838.51
space group	$P2_1/n$ (No. 14)	$P\bar{1}$ (No. 2)	*Pbca* (No. 61)
a, Å	16.207(3)	9.995(2)	20.835(4)
b, Å	15.680(3)	10.412(2)	19.457(4)
c, Å	11.245(2)	14.327(2)	16.096(3)
α, deg		104.88(1)	
β, deg	92.24(1)	103.83(1)	
γ, deg		92.51(1)	
V, Å^3	2855.5(9)	1390.4(5)	6525(2)
T, °C	22	20	26
Z	4	2	8
ρ_{calc}, g cm^{-3}	1.562	1.676	1.707
μ, cm^{-1}	7.07	7.37	7.09
θ range, deg	2–25	2–27	2–23
data limits	$\pm h,k,l$	$h\pm k,\pm l$	$h,k,\pm l$
no. of data collcd	5532	7711	7256
no. of unique data	5024	6074	4525
transm coeff		0.86–0.95	0.84–0.94
no. of data refined	3746	4948	2383
no. of LS params	356	403	428
R^a	0.034	0.033	0.051
R_w^b	0.038	0.038	0.055

^{a} $R = \sum\|F_o\| - |F_c\|/\sum|F_o|$. ^{b} $R_w = [\sum w(|F_o| - |F_c|)^2/\sum w|F_o|^2]^{1/2}$.

(12) Sheldrick, G. M. SHELX76: Program for Crystal Structure Determination. University of Cambridge, Cambridge, UK, 1976.

(13) Hall, S. R.; Stuart, J. M. XTAL3.0: Reference Manual. University of Western Australia, and University of Maryland, 1990.

Table II. Final Atomic Coordinates and Equivalent Thermal Displacement Parameters (Å²) for $[Ru(\eta^5\text{-}C_5H_4PCy_3)(\eta^5\text{-}C_5H_4OH)]PF_6$ (**7**)

	x/a	y/b	z/c	U_{eq}[a]		x/a	y/b	z/c	U_{eq}[a]
Ru	0.53644(2)	0.04019(2)	0.25739(3)	0.0374(1)	C(17)	0.6174(2)	0.2795(2)	0.1139(3)	0.031(1)
P(1)	0.55919(5)	0.26939(5)	0.24763(7)	0.0276(2)	C(18)	0.6557(2)	0.3672(2)	0.0920(3)	0.043(1)
C(1)	0.5010(2)	0.1730(2)	0.2282(3)	0.032(1)	C(19)	0.6953(2)	0.3675(2)	−0.0281(3)	0.047(1)
C(2)	0.4471(2)	0.1343(2)	0.3099(3)	0.040(1)	C(20)	0.7574(2)	0.2971(3)	−0.0381(3)	0.052(1)
C(3)	0.4040(2)	0.0674(3)	0.2503(4)	0.053(1)	C(21)	0.7199(3)	0.2107(3)	−0.0142(3)	0.052(1)
C(4)	0.4301(2)	0.0621(2)	0.1330(4)	0.052(1)	C(22)	0.6824(2)	0.2097(2)	0.1074(3)	0.043(1)
C(5)	0.4893(2)	0.1271(2)	0.1175(3)	0.040(1)	C(23)	0.6304(2)	0.2683(2)	0.3801(3)	0.037(1)
C(6)	0.6619(2)	0.0185(3)	0.3392(4)	0.051(1)	C(24)	0.6628(2)	0.3584(3)	0.4116(3)	0.053(1)
C(7)	0.6031(3)	−0.0190(3)	0.4093(4)	0.057(2)	C(25)	0.7303(3)	0.3531(3)	0.5111(4)	0.069(2)
C(8)	0.5617(3)	−0.0832(3)	0.3390(4)	0.064(2)	C(26)	0.7007(3)	0.3092(3)	0.6193(4)	0.070(2)
C(9)	0.5951(3)	−0.0824(3)	0.2240(4)	0.061(2)	C(27)	0.6658(3)	0.2214(3)	0.5896(4)	0.068(2)
C(10)	0.6561(3)	−0.0180(3)	0.2255(4)	0.054(2)	C(28)	0.5980(2)	0.2242(2)	0.4901(3)	0.044(1)
O(1)[b]	0.7176(3)	0.0713(3)	0.3790(4)	0.065(2)	P(2)	0.92309(7)	0.14349(7)	0.2616(1)	0.0530(3)
O(2)[b]	0.709(1)	0.002(1)	0.146(2)	0.092(8)	F(1)	0.9860(2)	0.1044(3)	0.1800(3)	0.157(2)
C(11)	0.4865(2)	0.3575(2)	0.2524(3)	0.030(1)	F(2)	0.8579(2)	0.1824(3)	0.3420(3)	0.138(2)
C(12)	0.4392(2)	0.3626(2)	0.3664(3)	0.038(1)	F(3)	0.8995(2)	0.2114(2)	0.1631(3)	0.100(1)
C(13)	0.3833(2)	0.4403(2)	0.3628(3)	0.044(1)	F(4)	0.9468(2)	0.0743(2)	0.3588(3)	0.109(1)
C(14)	0.3239(2)	0.4400(2)	0.2530(3)	0.048(1)	F(5)	0.9886(2)	0.2053(2)	0.3205(4)	0.158(2)
C(15)	0.3699(2)	0.4329(2)	0.1403(3)	0.049(1)	F(6)	0.8538(2)	0.0837(2)	0.2050(3)	0.128(2)
C(16)	0.4258(2)	0.3548(2)	0.1427(3)	0.043(1)					

[a] $U_{eq} = {}^1/_3 \sum_i \sum_j U_{ij} a_i^* a_j^* (a_i a_j)$. [b] Alternately occupied sites; site occupation factors 0.76(1) for O(1), and 0.24(1) for O(2).

Table III. Final Atomic Coordinates and Equivalent Thermal Displacement Parameters (Å²) for $[Ru(\eta^5\text{-}C_5H_5)(\eta^4\text{-}C_5H_4O)(P(OPh)_3)]PF_6$ (**13**)

	x/a	y/b	z/c	U_{eq}[a]		x/a	y/b	z/c	U_{eq}[a]
Ru	0.20718(2)	0.19330(2)	0.29465(2)	0.03465(7)	C(20)	0.1707(4)	−0.4227(3)	0.0223(3)	0.062(1)
C(1)	0.3966(3)	0.2167(3)	0.4165(2)	0.053(1)	C(21)	0.1596(4)	−0.3418(3)	0.1112(3)	0.061(1)
C(2)	0.3206(4)	0.3234(3)	0.4438(2)	0.059(1)	C(22)	0.1956(3)	−0.2044(3)	0.1370(2)	0.048(1)
C(3)	0.1922(4)	0.2681(4)	0.4508(2)	0.061(1)	C(23)	0.5756(3)	−0.0324(3)	0.2283(2)	0.038(1)
C(4)	0.1901(4)	0.1274(4)	0.4279(2)	0.059(1)	C(24)	0.6712(3)	−0.0485(3)	0.3088(2)	0.047(1)
C(5)	0.3149(4)	0.0945(3)	0.4060(2)	0.056(1)	C(25)	0.7900(3)	−0.1067(3)	0.2935(3)	0.057(1)
C(6)	0.0888(3)	0.2094(3)	0.1122(2)	0.043(1)	C(26)	0.8081(3)	−0.1467(3)	0.1993(3)	0.057(1)
C(7)	0.1281(3)	0.3282(3)	0.1981(2)	0.048(1)	C(27)	0.7114(3)	−0.1282(3)	0.1191(3)	0.058(1)
C(8)	0.0448(3)	0.3188(3)	0.2622(2)	0.050(1)	C(28)	0.5927(3)	−0.0702(3)	0.1333(2)	0.050(1)
C(9)	−0.0165(3)	0.1828(3)	0.2354(2)	0.048(1)	P(2)	0.1523(1)	0.71589(9)	0.43493(7)	0.0594(4)
C(10)	0.0283(3)	0.1109(3)	0.1549(2)	0.044(1)	F(1)[b]	0.0738(3)	0.8351(3)	0.4818(3)	0.109(2)
O(1)	0.1044(2)	0.1941(2)	0.0288(2)	0.0566(9)	F(2)[b]	0.2260(4)	0.6008(3)	0.3819(4)	0.145(3)
P(1)	0.34343(7)	0.09464(7)	0.19035(5)	0.0339(3)	F(3)[b]	0.2933(3)	0.8137(4)	0.4749(4)	0.128(2)
O(2)	0.4222(2)	0.1830(2)	0.1399(1)	0.0411(7)	F(4)[b]	0.0111(5)	0.6331(5)	0.4000(5)	0.176(3)
O(3)	0.2770(2)	−0.0150(2)	0.0870(1)	0.0401(7)	F(5)[b]	0.1268(8)	0.7771(7)	0.3407(4)	0.126(4)
O(4)	0.4580(2)	0.0252(2)	0.2513(1)	0.0446(8)	F(6)[b]	0.169(1)	0.678(1)	0.5322(8)	0.243(8)
C(11)	0.4940(3)	0.3116(3)	0.1893(2)	0.043(1)	F(46)[b]	0.088(1)	0.597(1)	0.4689(8)	0.101(2)*
C(12)	0.6097(3)	0.3291(3)	0.2663(2)	0.051(1)	F(35)[b]	0.213(1)	0.803(1)	0.3871(9)	0.101(2)*
C(13)	0.6816(4)	0.4559(4)	0.3085(3)	0.068(2)	F(45)[b]	0.031(1)	0.656(1)	0.3319(7)	0.101(2)*
C(14)	0.6366(5)	0.5603(4)	0.2736(3)	0.084(2)	F(36)[b]	0.269(1)	0.743(1)	0.5244(8)	0.101(2)*
C(15)	0.5209(5)	0.5407(4)	0.1958(4)	0.087(2)	F(16)[b]	0.148(2)	0.765(2)	0.552(1)	0.101(2)*
C(16)	0.4467(4)	0.4147(3)	0.1509(3)	0.064(2)	F(25)[b]	0.166(2)	0.653(2)	0.338(1)	0.101(2)*
C(17)	0.2425(3)	−0.1524(3)	0.0705(2)	0.037(1)	F(26)[b]	0.271(2)	0.624(2)	0.482(1)	0.101(2)*
C(18)	0.2555(3)	−0.2319(3)	−0.0198(2)	0.048(1)	F(15)[b]	0.071(2)	0.818(1)	0.414(1)	0.101(2)*
C(19)	0.2194(4)	−0.3679(3)	−0.0435(3)	0.062(1)					

[a] See footnote *a* of Table II. [b] PF_6 group orientationally disordered. Refined site occupation factors 0.84(1) for F(1) and F(2), 0.77(1) for F(3) and F(4), 0.58(1) for F(5) and F(6), 0.28(1) for F(46) through F(36), and 0.18(1) for F(16) through F(15). Fluorine atom labels with two digits indicate positions between fluorine atoms with one digit labels. Asterisks indicate isotropic temperature factors.

position of the Ru atom. The remaining atoms were located in succeeding difference Fourier syntheses. Disorder was encountered for the oxygen atom of the cyclopentadienyl moiety, 75% of which was attached to ring carbon C(6) and the remainder to the neighboring ring carbon C(10). Hydrogen atoms were generated geometrically (C–H = 0.96 Å) and fixed relative to the atom to which they were bonded. The structure was refined by full matrix least-squares, minimizing $\sum w(|F_o| - |F_c|)^2$ where $w = 1/(\sigma^2(F_o) + 0.0002\,F_o^2)$, and applying a secondary extinction correction (final coefficient = 0.00028(5)). Final positional parameters are given in Table II.

$[Ru(\eta^5\text{-}C_5H_5)(\eta^4\text{-}C_5H_4O)(P(OPh)_3)]PF_6$ (13). A yellow crystal measuring 0.11 × 0.30 × 0.74 mm was used for data collection. An analytical absorption correction was applied to the data (Gaussian integration method, program SHELX76). The structure was solved by a Patterson synthesis and succeeding difference Fourier syntheses. Hydrogen atoms were generated geometrically (C–H = 0.96 Å) and fixed relative to the atom to which they were bonded. Disorder was encountered for the PF_6^- group. With a unique P atom in common, one major and two subordinate alternative orientations of the PF_6^- octahedra could be derived from difference Fourier syntheses. Serious parameter oscillations for these fluorine atoms during least-squares refinement were overcome by restraining distances, thermal displacement factors, and site population factors. The structure was refined by full matrix least-squares, minimizing $\sum w(|F_o| - |F_c|)^2$ where $w = 1/(\sigma^2(F_o) + 0.0002\,F_o^2)$, and applying a secondary extinction correction (final coefficient = 0.00071(15)). Final positional parameters are given in Table III.

$[Ru(\eta^5\text{-}C_5H_5)(\eta^4\text{-}C_5H_3O\text{-}2\text{-}PPh_3)(CH_3CN)](PF_6)_2$ (18). A brown crystal of approximate dimensions 0.09 × 0.30 × 0.31 mm was used for data collection. The scattering power of this crystal was relatively poor, and thus, the number of reflections with significant intensity was low (Table I). An analytical absorption correction was applied to the data (Gaussian integration method, program SHELX76). The structure was solved using direct methods, which revealed the position of the Ru atom. The remaining atoms were located in succeeding difference Fourier syntheses. Hydrogen atoms were generated geometrically (C–H = 0.96 Å) and fixed relative to the atom to which they were bonded. The orientation of the CH_3 group of the acetonitrile residue was obtained by refining it as a rigid group. High thermal displacement effects were encountered for the two independent PF_6^- anions. The structure was refined by full matrix least-squares, minimizing $\sum w(|F_o| - |F_c|)^2$ where $w = 1/(\sigma^2(F_o) + 0.0002\,F_o^2)$, and applying a secondary extinction correction

Table IV. Final Atomic Coordinates and Equivalent Thermal Displacement Parameters (Å²) for $[Ru(\eta^5\text{-}C_5H_5)(\eta^4\text{-}C_5H_3O\text{-}PPh_3)(MeCN)](PF_6)_2$ (**18**)

	x/a	y/b	z/c	U_{eq}[a]		x/a	y/b	z/c	U_{eq}[a]
Ru	0.19813(3)	0.53595(3)	0.54451(4)	0.0414(2)	C(22)	0.3510(4)	0.4100(5)	0.4850(6)	0.051(4)
C(1)	0.1580(8)	0.4692(7)	0.6430(7)	0.081(5)	C(23)	0.3878(4)	0.5643(5)	0.5866(6)	0.048(4)
C(2)	0.2148(7)	0.4954(7)	0.6699(7)	0.074(6)	C(24)	0.4017(5)	0.5092(6)	0.6380(7)	0.063(4)
C(3)	0.2075(7)	0.5663(7)	0.6738(6)	0.077(6)	C(25)	0.4165(6)	0.5188(7)	0.7199(7)	0.081(6)
C(4)	0.1456(8)	0.5817(6)	0.6464(7)	0.081(6)	C(26)	0.4185(6)	0.5831(8)	0.7525(8)	0.090(6)
C(5)	0.1145(6)	0.5203(8)	0.6252(7)	0.080(6)	C(27)	0.4068(6)	0.6387(7)	0.7013(9)	0.089(6)
C(6)	0.2411(5)	0.5508(5)	0.3958(6)	0.051(4)	C(28)	0.3918(5)	0.6309(6)	0.6179(7)	0.069(5)
C(7)	0.2820(4)	0.5726(4)	0.4691(5)	0.040(3)	N(1)	0.1977(4)	0.4435(4)	0.4815(5)	0.050(3)
C(8)	0.2492(5)	0.6266(5)	0.5095(6)	0.050(4)	C(29)	0.1969(5)	0.3928(6)	0.4496(7)	0.064(4)
C(9)	0.1862(5)	0.6319(5)	0.4752(7)	0.063(5)	C(30)	0.1948(6)	0.3254(5)	0.4090(8)	0.090(5)
C(10)	0.1777(5)	0.5824(6)	0.4183(6)	0.057(4)	P(2)	0.2184(1)	0.7863(2)	0.6966(2)	0.063(1)
O(1)	0.2562(3)	0.5149(4)	0.3379(4)	0.072(3)	F(1)	0.2590(5)	0.7216(4)	0.7071(6)	0.175(5)
P(1)	0.3650(1)	0.5521(1)	0.4798(1)	0.0424(8)	F(2)	0.1785(4)	0.8509(4)	0.6806(6)	0.163(5)
C(11)	0.4119(5)	0.6079(4)	0.4157(6)	0.047(4)	F(3)	0.1834(7)	0.7518(5)	0.6280(8)	0.251(7)
C(12)	0.4741(5)	0.6240(5)	0.4344(7)	0.059(4)	F(4)	0.2528(7)	0.8200(5)	0.7617(9)	0.266(8)
C(13)	0.5119(5)	0.6597(6)	0.3792(7)	0.068(5)	F(5)	0.2602(7)	0.8156(8)	0.634(1)	0.30(1)
C(14)	0.4866(6)	0.6793(6)	0.3032(7)	0.068(5)	F(6)	0.1741(7)	0.7604(8)	0.753(1)	0.299(9)
C(15)	0.4245(6)	0.6656(6)	0.2844(7)	0.082(5)	P(3)	-0.0150(2)	0.6614(2)	0.4810(3)	0.089(2)
C(16)	0.3860(5)	0.6297(5)	0.3397(6)	0.064(4)	F(7)	0.0457(4)	0.6826(6)	0.5247(8)	0.222(7)
C(17)	0.3790(4)	0.4657(5)	0.4450(6)	0.045(3)	F(8)	-0.0757(5)	0.6469(6)	0.4317(7)	0.208(6)
C(18)	0.4167(5)	0.4536(5)	0.3739(6)	0.054(4)	F(9)	-0.0509(5)	0.7070(8)	0.540(1)	0.264(9)
C(19)	0.4244(5)	0.3876(7)	0.3461(7)	0.068(5)	F(10)	0.0213(5)	0.6120(7)	0.431(1)	0.288(9)
C(20)	0.3978(5)	0.3334(6)	0.3875(8)	0.064(5)	F(11)	-0.0358(7)	0.6056(7)	0.5360(8)	0.256(8)
C(21)	0.3611(5)	0.3450(5)	0.4562(7)	0.066(4)	F(12)	-0.0044(8)	0.7206(8)	0.425(1)	0.32(1)

[a] See footnote *a* of Table II.

(final coefficient = 0.00003(1)). Final positional parameters are given in Table IV.

Results

Reactions of 1 and 2 with Tertiary Phosphines, Phosphites, and Arsines. When a nitromethane solution of **1** is treated with PR_3 (R = Me, Cy, Ph) or $AsMe_3$, the red solution rapidly turns pale yellow. In each case substitution takes place exclusively on the C_5H_5 ring, the ketone being reduced to the alcohol, η^5-C_5H_4OH (reaction 3). By use of ^1H NMR spectroscopy on the product

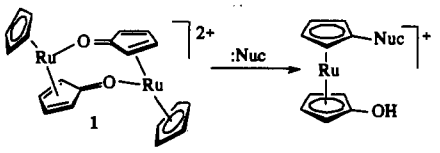

(3)

:Nuc = PMe_3 (**6**), PCy_3 (**7**), PPh_3 (**8**), $AsMe_3$ (**10**)

solutions (CD_3NO_2 or $(CD_3)_2CO$), the reactions were found to be essentially quantitative; the recovered yields are typically 50–60%. All products are air stable.

The ^1H and ^{13}C NMR spectra of the various complexes reveal the same overall resonance pattern diagnostic for 1,1′-disubstituted ruthenocenes. The α and β protons of η^5-C_5H_4OH give rise to two apparent triplets, and the α and β protons of η^5-$C_5H_4PR_3$ and η^5-$C_5H_4AsMe_3$, respectively, reveal two apparent multiplets. The ^{13}C NMR spectra exhibit a characteristic singlet assigned to the resonances of the "hydroxy" carbon at 128.0, 127.8, 129.0, and 127.9 ppm in **6**, **7**, **8**, and **10**, respectively. Furthermore, short and long range ^{13}C–^{31}P coupling in η^5-$C_5H_4PR_3$ results in the appearance of three doublets aside from the signals of the phosphine moiety. The IR spectra in KBr show a strong absorption in the range of 1520–1513 cm^{-1} characteristic of the C–O stretching frequency. A structural view of **7** as determined by X-ray diffraction is depicted in Figure 1.

With **2** as starting material only in the case of the tertiary alkyl phosphines PMe_3 and PCy_3 were the same products as for **1** obtained. As established by ^1H and ^{13}C NMR spectroscopy (reaction 4), PPh_3 reacts with **2** by substituting solely on the cyclopentadienone ligand to give **9**. The ^1H NMR spectrum of **9** recorded in $(CD_3)_2CO$ consists of five signals: a multiplet pattern from 8.00–7.78 ppm (15H), three multiplets centered at 5.21

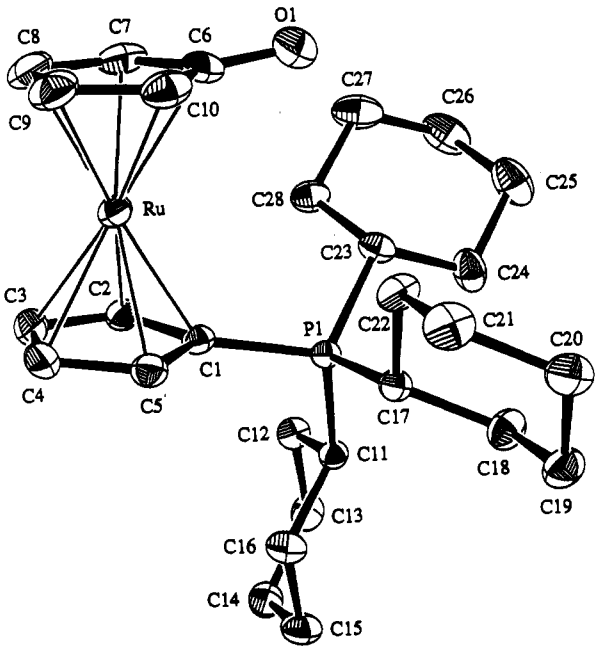

Figure 1. Structural view of $[Ru(\eta^5\text{-}C_5H_4PCy_3)(\eta^5\text{-}C_5H_4OH)]PF_6$ (**7**).

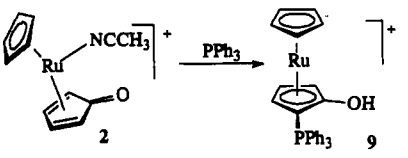

(4)

(1H), 4.76 (1H), and 4.16 ppm (1H), and a singlet at 4.57 ppm (5H). The resonance of the OH proton was not observed. Due to the coupling with ^{31}P of the phosphine moiety, the ^{13}C resonances of the disubstituted ring are split into doublets, including the resonance of the "hydroxy" carbon observed at 129.4 ppm (J_{CP} = 7.0 Hz). The singlet at 74.5 ppm is assigned to the unsubstituted C_5H_5 ring. The C–O stretching frequency was found at 1520 cm^{-1}.

Reaction of **2** with $AsMe_3$ results in the formation of **11** as the major product (reaction 5). **11** was characterized by ^1H and ^{13}C NMR spectroscopy and elemental analysis. The characteristic

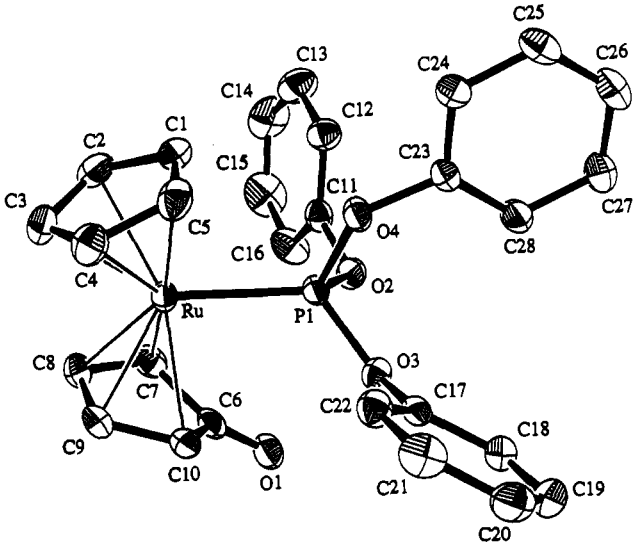

Figure 2. Structural view of $[Ru(\eta^5\text{-}C_5H_5)(\eta^4\text{-}C_5H_4O)(P(OPh)_3)]PF_6$ (**13**).

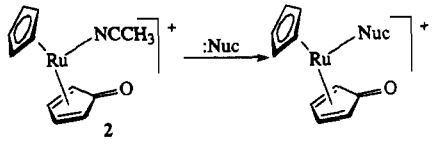

(5)

:Nuc = $AsMe_3$ (**11**), $AsPh_3$ (**19**), $P(OPh)_3$ (**13**)

resonance of the "carbonyl" carbon was observed at 181.6 ppm. By use of ^1H NMR spectroscopy on the product solution in CD_3NO_2 it was found that this reaction produced a second complex (**12**) in yields of about 5%. This species could not be isolated but its structure was assigned by ^1H NMR spectroscopy (see Experimental Section).

$P(OPh)_3$ reacts both with **1** and **2** exclusively by substituting on the metal center giving **13** in 92% isolated yield (reaction 5). The appearance of two apparent multiplets at 6.16 (2H) and 3.77 ppm (2H) and a sharp singlet at 5.70 ppm (5H), along with the peak integrations, establishes the identity of this complex. Furthermore, the ^{13}C NMR spectrum of **13** displays a singlet at 183.6 ppm (C=O). An X-ray crystal structure of **13** was determined. The molecular structure of **13** is shown in Figure 2. Synthesis and spectroscopic properties of **19** have been reported recently.[7]

Treatment of **1** with $P(OMe)_3$ resulted in the rapid decomposition of the starting material as monitored by ^1H NMR spectroscopy. Among the decomposition products observed by ^1H NMR spectroscopy were two 1,1′-disubstituted ruthenocenes as indicated by the presence of two sets of apparent triplets and two sets of apparent multiplets, respectively. The ^{13}C NMR spectrum, though otherwise relatively uninformative, contained peaks at 129.5 and 123.1 ppm, respectively, indicative of the presence of $\eta^5\text{-}C_5H_4OH$ ligands. Moreover, the presence of several doublets in the range of 80–60 ppm revealed that some phosphorus-containing moiety was introduced to the C_5H_5 ring. There was, however, no indication of $P(OMe)_3$ being the substituent. We were not able yet to assign the structure of these substituents. All attempts to isolate and identify these compounds were unsuccessful.

Reaction of 8 with Propionyl Chloride. To illustrate the procedure a representative ester (**14**) has been prepared in 54% yield by the action of propionyl chloride in the presence of triethylamine on **8**. Its identity was established by ^1H NMR spectroscopy and elemental analysis.

Reactions of 8 and 9 with Br_2, I_2, Ag^+, and $[Fe(\eta^5\text{-}C_5H_5)_2]^+$. Treatment of **8** with Br_2 resulted in the formation of **15**, the

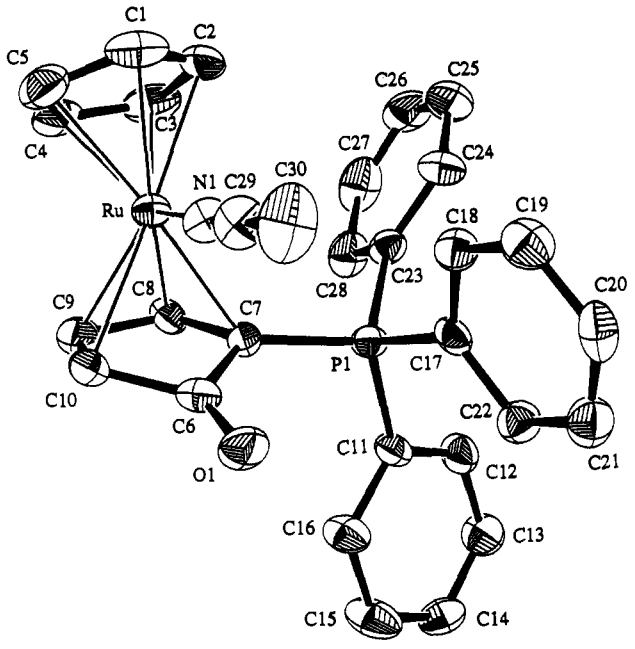

Figure 3. Structural view of $[Ru(\eta^5\text{-}C_5H_5)(\eta^4\text{-}C_5H_3O\text{-}2\text{-}PPh_3)(MeCN)](PF_6)_2$ (**18**).

C_5H_4OH ring being converted quantitatively to the corresponding ketone (reaction 6). Though **15** could not be isolated as a solid,

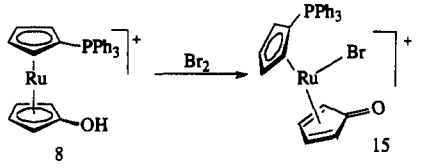

(6)

its structure was determined by ^1H and ^{13}C NMR spectroscopy. Indicative of the formation of **15** was the resonance of the "carbonyl" carbon observed at 179.3 ppm. The weaker oxidizing agents I_2 and Ag^+ are not able to oxidize **8**.

In analogy to **8**, **9** is readily oxidized by Br_2 to give **16** in 79% isolated yield (reaction 7). The ^1H NMR spectrum of **16** shows

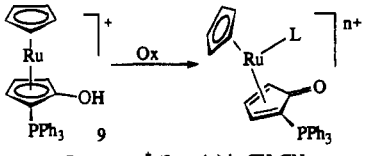

(7)

Ox = Br_2, I_2, Ag^+ (2 equiv) in CH_3CN
L = Br^- (**16**), I^- (**17**); n = 1
L = CH_3CN (**18**); n = 2

the same overall pattern as that of **9**. However, all signals are considerably shifted downfield. The signal of the "carbonyl" carbon in the ^{13}C NMR spectrum of **16** is observed at 180.8 ppm. The IR spectrum displays the expected peak for the C=O stretching frequency at 1690 cm^{-1}. Iodine and Ag^+, introduced as the PF_6^- salt in CH_3CN as a solvent, react with **9** to yield analogous products (reaction 7). However, longer reaction times are necessary in order to convert **9** quantitatively to **17** and **18**, respectively. Since **18** appears to be the first dicationic complex with a monosubstituted cyclopentadienone, its molecular structure was determined by X-ray crystallography and is depicted in Figure 3. This structure also established that regioselective attack of PPh_3 in the position α to the ketonic group in **2** had occurred. In contrast to Br_2, I_2, and Ag^+, the ferrocenium cation does not react with **9**.

Reactions of $[Ru(\eta^5\text{-}C_5H_5)(\eta^4\text{-}C_5H_4O)L]^+$ (L = SEt_2 (3), NC_5H_5 (4), Br^- (5)) with PPh_3. Treatment of **3** with PPh_3 (1

equiv) results in the slow formation of **9** as shown by ^{1}H NMR spectroscopy. After 1 week about 60% of **3** had been converted to **9**. No side products could be detected.

In contrast to **3**, both **4** and **5** react readily with PPh_3 to give a complex identified as hydroxyruthenocene. This complex was also prepared recently by the action of Zn or NaHg on **5**.[14] The ^{1}H NMR spectra exhibits apparent triplets at 4.53 (2H) and 4.12 ppm (2H), respectively, and a singlet at 4.47 ppm (5H). There was no evidence, however, that PPh_3 was introduced into the C_5H_5 and/or C_5H_4O rings. A $^{31}P\{^1H\}$ NMR spectrum of the reaction mixture of **5** and PPh_3 was recorded and exhibited several singlets shifted down field to 66.9, 47.2, 42.7, and 31.7 ppm, respectively, with respect to PPh_3.

Crystal Structure of $[Ru(\eta^5\text{-}C_5H_4PCy_3)(\eta^5\text{-}C_5H_4OH)]PF_6$ (7). The structure of the cation is shown in Figure 1. The five-membered rings are nearly parallel to one another, the angle between the two planes being 3.5(2)°. The rings adopt an eclipsed conformation. Both OH and PCy_3 groups deviate from the cyclopentadienyl planes, in that O(1) and P(1) are bent away from the metal and are located 0.230(6) and 0.182(1) Å out of the ring planes, corresponding to a respective tilt of 7.4(2) and 8.1(4)°, respectively. The Ru–C distances are all similar, averaging to 2.189(4) Å, and can be compared to the Ru–C distances of $Ru(\eta^5\text{-}C_5H_5)_2$ (2.21 Å)[15] and $[Ru(\eta^5\text{-}C_5H_5)_2I]^+$ (2.20(2) Å).[16] There is a clear trend in the delocalized C–C bond distances within $C_5H_4PCy_3$ varying from 1.428(5) and 1.443(5) Å (C(1)–C(2) and C(5)–C(1), respectively) to 1.403(6) Å (C(3)–C(4)). The C–C distances in the C_5H_4OH ligand (average 1.421(5) Å) do not show this effect. In parent ruthenocene the average C–C distance is 1.43 Å.[15] The C(6)–O(1) distance is 1.292(6) Å and the P(1)–C(1) distance is 1.790(3) Å. The C_5H_4OH ring exhibits a disorder of the OH group with a site occupancy of 75% for O(1) being attached to C(6) and a site occupancy of 25% for O(2) being attached to the neighboring ring carbon C(10). In both orientations the hydroxy groups appear to be hydrogen bonded (O–H···F) to the PF_6^- anion. The cyclohexyl rings adopt the usual chair conformation. Selected bond distances may be found in Table V.

Crystal Structure of $[Ru(\eta^5\text{-}C_5H_5)(\eta^4\text{-}C_5H_4O)(P(OPh)_3)]PF_6$ (13). An ORTEP view of **13** is presented in Figure 2. The C_5H_5 and C_5H_4O rings are approximately staggered with respect to one another. The C_5H_4O ligand is distinctly bent and can be subdivided into two planes, one defined by C(7), C(8), C(9), and C(10) (butadiene fragment) and the other defined by C(7), C(6), O(1), and C(10). The angle between these planes is 23.7(2)° and somewhat larger than commonly encountered in complexes containing C_5H_4O as a ligand. In $Fe(\eta^4\text{-}C_5H_4O)(CO)_3$, $[Mo(\eta^5\text{-}C_5H_5)(\eta^4\text{-}C_5H_4O)(CO)_2]^+$, $[Ru(\eta^5\text{-}C_5H_5)(\eta^4\text{-}C_5H_4O)(CH_3CN)]^+$ (**2**), and $Ru(\eta^5\text{-}C_5H_5)(\eta^4\text{-}C_5H_4O)Br$ (**5**) this angle is 19.9, 18.0, 18.0, and 20.6°, respectively.[3-5,7] The diene C–C bonds adopt a short–long–short pattern (1.392(4) vs 1.450(4) Å) as was the case for the complexes mentioned above. The angle between the C_5H_5 plane and the butadiene fragment of C_5H_4O is 36.5(2)° (for comparison in **2** and **5** it is 36.0 and 36.2°, respectively).[4,6] The average Ru–C(C_5H_5) distance is 2.214(3) Å. The bond distances between Ru and the butadiene fragment are short for C(8) and C(9) being 2.167(3) and 2.181(3) Å, respectively, and long for C(7) and C(10) being 2.255(3) and 2.283(3) Å, respectively. The lengths of the C(6)–O(1) and Ru–P(1) bonds are 1.212(4) and 2.335(1) Å, respectively. The C–O distance is comparable to the corresponding distances in $Fe(\eta^4\text{-}C_5H_4O)(CO)_3$, $[Mo(\eta^5\text{-}C_5H_5)(\eta^4\text{-}C_5H_4O)(CO)_2]^+$, **2**, and **5** being 1.224(9), 1.212(4), 1.221(7), and 1.22(1) Å, respectively.[3-5,7] Selected bond distances may be found in Table V.

(14) Kirchner, K.; Kwan, K. S.; Taube, H. *Inorg. Chem.*, in press.
(15) Hardgrove, G. L.; Templeton, D. H. *Acta Crystallogr.* **1959**, *12*, 28.
(16) Sohn, Y. S.; Schlueter, A. W.; Hendrickson, D. N.; Gray, H. B. *Inorg. Chem.* **1974**, *13*, 301.

Table V. Selected Bond Lengths (Å)

	7	13	18
Ru–C(1)	2.182(3)	2.203(3)	2.214(13)
Ru–C(2)	2.165(3)	2.215(3)	2.195(11)
Ru–C(3)	2.187(4)	2.215(3)	2.173(10)
Ru–C(4)	2.204(4)	2.227(4)	2.163(13)
Ru–C(5)	2.195(3)	2.209(4)	2.195(12)
Ru–C(6)	2.224(4)		
Ru–C(7)	2.191(4)	2.255(3)	2.245(8)
Ru–C(8)	2.174(4)	2.167(3)	2.135(9)
Ru–C(9)	2.183(4)	2.181(3)	2.189(10)
Ru–C(10)	2.186(4)	2.283(3)	2.263(10)
Ru–P(1)		2.335(1)	
Ru–N(1)			2.064(7)
C(1)–C(2)	1.428(5)	1.400(5)	1.360(20)
C(2)–C(3)	1.416(5)	1.420(5)	1.390(20)
C(3)–C(4)	1.403(6)	1.415(5)	1.397(21)
C(4)–C(5)	1.416(5)	1.393(5)	1.401(19)
C(5)–C(1)	1.443(5)	1.436(5)	1.375(20)
C(6)–C(7)	1.391(6)	1.465(4)	1.516(13)
C(7)–C(8)	1.431(6)	1.397(4)	1.412(12)
C(8)–C(9)	1.421(7)	1.435(4)	1.428(14)
C(9)–C(10)	1.413(6)	1.387(4)	1.340(15)
C(10)–C(6)	1.400(6)	1.496(5)	1.500(14)
C(6)–O(1)	1.292(6)	1.212(4)	1.208(12)
P(1)–C(1)	1.790(3)		
P(1)–C(7)			1.782(8)
P(1)–C(11)	1.818(3)		1.789(9)
P(1)–C(17)	1.813(3)		1.796(10)
P(1)–C(23)	1.849(3)		1.799(9)
P(1)–O(2)		1.593(2)	
P(1)–O(3)		1.591(2)	
P(1)–O(4)		1.586(2)	
N(1)–C(29)			1.113(13)
C(29)–C(30)			1.466(15)

Crystal Structure of $[Ru(\eta^5\text{-}C_5H_5)(\eta^4\text{-}C_5H_3O\text{-}2\text{-}PPh_3)(CH_3CN)](PF_6)_2$ (18). A structural view of **18** is displayed in Figure 3. Similar to the structure of **13**, in **18** the two C_5 rings adopt an approximately staggered conformation. The PPh_3 substituent is bound in α position to the ketonic group 7.6(5)° out of plane of the butadiene unit bent away from the metal, the P(1)–C(7) distance being 1.782(8) Å. Though the bond distances of **18** are less accurate than in **13**, the dienone character of C_5H_4O is still apparent as indicated by the short–long–short pattern of the C–C distances. The C–C distances of the C_5H_4O ring are almost identical to the respective distances in the parent complex (**2**). The angle between the plane defined by the atoms C(7), C(8), C(9), and C(10) and the carbonyl functionality C(6)–O(1) is 16.3(5)° (for comparison in **2** this angle is 18.0°),[7] and the ketonic group is bent away from the metal. The C(6)–O(1) distance is 1.208(12) Å (1.221(7) Å in **2**). The angle between the C_5H_5 plane and the butadiene fragment of C_5H_3O-2-PPh_3 is 35.5(7)°. Acetonitrile is coordinated in η^1-fashion and practically linear (angle between N(1)-C(29)-C(30) is 179(1)°). The Ru–N(1) distance is 2.064(7) Å (in **2** this distance is 2.057(5) Å).[7] Other selected bond angles are shown in Table V.

Discussion

Our work on **1** and **2** has shown that in these complexes the C_5H_5 moiety is unusually reactive toward certain nucleophiles. Thus the reactions of **1** with PR_3 (R = Me, Cy, Ph) and $AsMe_3$ yielding 1,1′-disubstituted ruthenocenes of the type $[Ru(\eta^5\text{-}C_5H_4PR_3)(\eta^5\text{-}C_5H_4OH)]PF_6$ and $[Ru(\eta^5\text{-}C_5H_4AsMe_3)(\eta^5\text{-}C_5H_4OH)]PF_6$, respectively (reaction 3), proceed readily at room temperature. Similarly, the reaction of **2** with the more basic phosphines PMe_3 and PCy_3 results in the formation of the analogous products. However, when PPh_3 reacts with **2** a different pattern is followed, attack occurring exclusively on the ketone to form $[Ru(\eta^5\text{-}C_5H_5)(\eta^5\text{-}C_5H_3OH\text{-}2\text{-}PPh_3)]PF_6$, (**9**), (reaction 4). Further, when **2** is treated with $AsMe_3$, the corresponding product resulting

from attack on the ketone ring is obtained in low yield, the major product being $[Ru(\eta^5\text{-}C_5H_5)(\eta^4\text{-}C_5H_4O)(AsMe_3)]PF_6$, **11**, (reaction 5). Remarkably, both **1** and **2** react with $P(OPh)_3$ and $AsPh_3$ solely by simple ligand substitution on the metal center to yield $[Ru(\eta^5\text{-}C_5H_5)(\eta^4\text{-}C_5H_4O)(P(OPh)_3)]PF_6$ (**13**) and $[Ru(\eta^5\text{-}C_5H_5)(\eta^4\text{-}C_5H_4O)(AsPh_3)]PF_6$ (**19**) (reaction 5), respectively.[7]

The reactivity of **1** and **2** toward nucleophilic attack on C_5H_5 and/or C_5H_4O appears to be largely dictated by two factors: (i) the strength of the nucleophile itself, and (ii) the ancillary ligand attached to the metal center. The nucleophilicity decreases in the order $PCy_3 > PMe_3 > PPh_3 > AsMe_3 \gg AsPh_3 \approx P(OPh)_3$. In the case of the phosphines and $P(OPh)_3$, the values as determined by the pK_a and heat of protonation (HP) values, respectively,[17,18] run parallel; for the arsines no pK_a and HP values are available.

On the basis of the relative HP data[18] the reactivity of $P(OMe)_3$ is expected to be comparable to that of PPh_3. ^1H and ^{13}C NMR spectroscopic data confirm that when $P(OMe)_3$ reacts with **1**, nucleophilic attack on C_5H_5 takes place, but we have no proof that $P(OMe)_3$ is the substituent.

The role of the ancillary ligand is demonstrated in the reactions of $[Ru(\eta^5\text{-}C_5H_5)(\eta^4\text{-}C_5H_4O)(SEt_2)]PF_6$ (**3**), $[Ru(\eta^5\text{-}C_5H_5)(\eta^4\text{-}C_5H_4O)(NC_5H_5)]PF_6$ (**4**), and $Ru(\eta^5\text{-}C_5H_5)(\eta^4\text{-}C_5H_4O)Br$ (**5**) with PPh_3. While, with **3**, substitution takes place on the cyclopentadienone ring to give **9**, compounds **4** and **5** form hydroxyruthenocene[14] with no evidence for ring substitution. Qualitatively, the reactivity of **1–5** toward nucleophilic attack falls in the sequence **1 > 2 > 3 > 4 > 5** and is discussed in more detail in the following paragraphs.

Formally, complexes **1–5** involve positive divalent oxidation states and, thus, on the basis of the 18e⁻ rule, structurally resemble the η^4-diene complex **I**.[19] ^1H and ^{13}C NMR resonances of C_5H_5

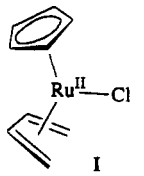

I

rings coordinated to Ru(II) are typically in the range of 4.5 and 85 ppm.[19]

It is, however, difficult to explain the reactivity pattern observed for **1** and **2** by invoking the above structure, which would lead to the expectation that nucleophilic attack would take place at cyclopentadienone rather than at C_5H_5.[8,20] In fact, cationic η^4-diene complexes are considered to be among the substrates most receptive to nucleophilic attack, this being favored at the terminal carbons, i.e., in the case of C_5H_4O in the position α to the ketonic group. This has indeed been demonstrated very recently by the reactions of $[Mo(CO)_2(\eta^5\text{-}C_5H_5)(\eta^4\text{-}C_5H_4O)]^+$ with various carbanions, which yield substituted η^3-cyclopentenoyl complexes (reaction 1).[5]

Nucleophilic substitution on coordinated $\eta^5\text{-}C_5H_5$, on the other hand, has been observed for the 4+ oxidation state metallocenes $[Ru(\eta^5\text{-}C_5H_5)_2X]^+$ (**II**). These, however, are not simple substitution reactions but involve the reduction of the metal center, with one C_5H_5 ring being converted to $\eta^4\text{-}C_5H_4O$.[4,7] The ^1H and ^{13}C NMR spectra of **II** show resonances for C_5H_5 at 6.07 and 94.9 ppm, respectively. The significant downfield shift compared to **I** is indicative of the electron-withdrawing power of Ru(IV),

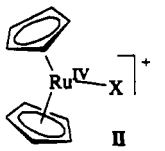

II

X = Cl⁻, Br⁻, I⁻

which ultimately leads to an increased reactivity of C_5H_5 in complexes **II**.[4]

These observations suggest that, in complexes containing the $[Ru(\eta^5\text{-}C_5H_5)(\eta^4\text{-}C_5H_4O)]^+$ moiety, there is a strong resonance interaction with the carbonyl group leading to the limiting structure **IIIb**. (In the case of complexes of the type of **2**, L

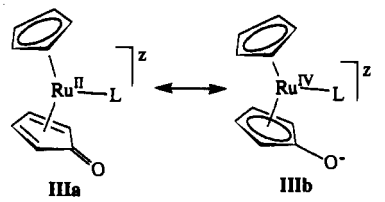

IIIa **IIIb**

L = CH_3CN or py; z = +
L = halide; z = 0

represents simple 2e⁻ donors such as CH_3CN, pyridine, or halides.) That there is an important contribution of **IIIb** to the ground state of **1** is suggested by the ^1H and ^{13}C NMR data, the resonances of C_5H_5 in **1** appearing at 6.09 and 95.8 ppm, respectively.[6,21] In the case of **1**, L is the oxygen atom of a second molecule, so that **IIIb** is stabilized relative to **IIIa** by the metal–O interaction.[7] The respective ^1H and ^{13}C NMR resonances for **2**, on the other hand, are shifted somewhat upfield and are observed at 5.64 and 87.8 ppm, respectively. The ^1H NMR spectra of **3**, **4**, and **5** exhibit slightly larger upfield shifts for the C_5H_5 resonances which are found at 5.62, 5.59, and 5.44 ppm, respectively, indicating that resonance hybrid **IIIa** figures more prominently than in **I**.

Additional support for a resonance interaction between the metal and the C_5H_4O ring stems from the X-ray structures of **1**, **2**, and **5**. In **IIIa** and **IIIb**, C_5H_4O is coordinated in η^4 and η^5 fashion, respectively. In the first binding mode the C=O functional group is out of plane from the butadiene fragment bent away from the metal, whereas in the latter a planar structure may be expected. The angle between the butadiene plane and the plane formed by the C=O group increases from 13.7 to 18.0 to 20.6° for **1**, **2**, and **5**, respectively.[4,7] This, in fact, is in line with the structural changes proposed on going from **IIIb** to **IIIa**.

The ^{13}C NMR resonances of the "carbonyl" carbons of **1–4**, though commonly considered as very structure sensitive,[22] exhibit only small upfield shifts observed at 183.3, 182.8, 182.3, and 181.6 ppm, respectively. In contrast, the ^{13}C resonances of "hydroxy" carbons are found in the range of approximately 128 ppm. Due to the low solubility of **5** in all common solvents no ^{13}C NMR spectrum could be obtained. The C=O stretching frequencies of **1–5** appear at 1569, 1699 (1684), 1672, 1682, and 1685 cm^{-1}, respectively.[7] A notable feature of the data is that the C=O absorption in **1** is shifted to a much lower frequency than is the case for the remainder.

The effects referred to above deal only with ground-state stabilization. To understand the reactivity patterns, electronic stabilization of the activated complexes must be taken into account—what is important is the change in electronic stabilization on activation. In the absence of kinetic data, even the composition of the activated complexes is as yet not defined dealing

(17) Golovin, M. N.; Rahman, Md. M.; Belemonte, J. E.; Giering, W. P. *Organometallics* **1985**, 4, 1981.
(18) Russell, C. B.; Angelici, R. J. *Inorg. Chem.* **1988**, *27*, 681.
(19) Albers, M. O.; Robinson, D. J.; Shaver, A.; Singleton, E. *Organometallics* **1986**, *5*, 2199.
(20) Collman, J. P.; Hegedus, L. S.; Norton, J. R.; Finke, R. G. in *Principles and Applications of Organotransitionmetal Chemistry*, 2nd ed.; University Science Books: Mill Valley, CA, 1987.
(21) The $^{13}C\{^1H\}$ NMR spectrum of **1** (δ, CD_3NO_2, −30 °C) shows peaks at 183.3 (C=O), 95.8 (C_5H_5), 94.4, 92.6, 89.6, 78.7; this has not been previously reported.
(22) Shvo, Y.; Czarkie, D.; Rahamim, Y.; Chodosh, D. F. *J. Am. Chem. Soc.* **1986**, *108*, 7400.

with this basic matter. For example, the participation of the ancillary ligands in the activation process is not established and this is a major issue. In the case of the reactions of **2**, does the nucleophile replace CH_3CN before attacking the rings, as it has been suggested?[7] Even if this does occur as the first step, does the ancillary ligand remain as a necessary part of the activated complex, or must it be ejected prior to reaction? This issue arises in trying to understand the difference in the way PPh_3 reacts with **1** (attack solely on C_5H_5) and with **2** (attack solely on the ketone). Presumably in the first step attack by PPh_3 takes place on a single member of the binuclear species. To explain the fact that the two reaction modes are exclusive, the entity resulting from attack on **1** cannot equilibrate to form the same mononuclear species which is intermediate in the case of **2**.

The present study has in fact exposed still an additional (fourth) mode of reaction which again is highly selective, exemplified by the reactions of **4** and **5** with PPh_3, which lead to the reduction of the ketone ring to form hydroxyruthenocene. The same product is obtained on the treatment of **5** with Zn or NaHg in tetrahydrofuran.[14] That PPh_3 can act as a reducing agent in an appropriate environment is no surprise. The $^{31}P\{^1H\}$ NMR spectrum of the reaction mixture of **5** and PPh_3 in CD_3NO_2 as a solvent exhibits several unidentified phosphorus resonances, all of them shifted down field with respect to PPh_3. Thus, the peak at 66.9 ppm may be ascribed to the formation of Ph_3PBr^+ (for comparison Ph_3PCl^+ in CD_2Cl_2 as a solvent shows a singlet at 65.3 ppm).[23] Also in the case of **4**, the latter issue has to be dealt with, but in addition, the identity of the product of the oxidation of PPh_3—specifically, the identity of the ligand which stabilizes P(V).

In connection with the reaction of PPh_3 with **2**, which involves exclusively regioselective attack on the ketone, it is interesting to compare the outcome to those reported recently for the reactions of carbanions with $[Mo(CO)_2(\eta^5\text{-}C_5H_5)(\eta^4\text{-}C_5H_4O)]^+$.[5] Though the same regioselectivity is found, the latter results in the formation of neutral η^3-cyclopentenoyl products (reaction 1). Depending on the oxidation state of the metal, i.e., Mo(I) or Mo(0), the allyl fragment of the C_5H_4O ring exhibits either an $\eta^3\text{-}C_3H_3^+$ or an $\eta^3\text{-}C_3H_3$-like behavior.

The different reactivity pattern observed for **2** and $[Mo(CO)_2(\eta^5\text{-}C_5H_5)(\eta^4\text{-}C_5H_4O)]^+$ can be attributed to the difference in the way the coligands CH_3CN and CO interact with the metal center. As the weaker π acid, CH_3CN, in contrast to CO, does not sufficiently stabilize lower oxidation states of the metal center in its particular ligand environment. Even the strong reducing agents Zn or NaHg acting on **2** do not yield products with Ru in lower oxidation states. Zerovalent Ru complexes of the type $[Ru(\eta^4\text{-}C_5R_4O)(CO)_3]$ (R = alkyl, aryl) with both CO and cyclopentadienones as ligands, however, do exist.[24-26]

In contrast to the action of PPh_3, those of $AsPh_3$ and of $P(OPh)_3$ result in simple ligand substitution on the metal. Thus, the different reactivity can not be explained on the basis of steric effects. In the case of $P(OPh)_3$ the low basicity of this ligand may account for the change in reactivity. It is, however, difficult to rationalize the striking reactivity difference between $AsPh_3$ and PPh_3 merely in terms of differing basicity.

Still yet to be addressed are the reactions of **8** and **9** with the following oxidizing agents, which have been ordered according to their potentials: $Br_2 > Ag^+/CH_3CN > I_2 > [Fe(\eta^5\text{-}C_5H_5)_2]^+$. Attempts to prepare Ru(IV) complexes by oxidation with Br_2 in analogy to parent ruthenocene failed. Instead, $\eta^5\text{-}C_5H_4OH$ was readily converted to the corresponding ketone resulting in the formation of **15** and **16**, respectively (reactions 6 and 7). It may be that a complex of Ru(IV) with $\eta^5\text{-}C_5H_4OH$ is inherently unstable to the internal redox process. Treatment of **8** and **9** with the weaker oxidizing agents I_2 and Ag^+/CH_3CN in the case of **9** resulted in the formation of **17** and **18**, whereas with **8** no reaction occurred. Ferrocenium does not oxidize **9**, but whether this is because the reaction is slow (note that 2 equiv of $[Fe(\eta^5\text{-}C_5H_5)_2]^+$ are required for the oxidation of the alcohol) or because the equilibrium is unfavorable is not known. Salts of **16** and **18** were isolated in pure form and appear to be the first cationic complexes with a monosubstituted cyclopentadienone ligand. The molecular structure of **18** has been determined by X-ray crystallography (Figure 3). It has to be noted that **18** was prepared also by the action of Ag^+ on **16** in CH_3CN as a solvent.

Acknowledgment. Financial support by the "Fonds zur Förderung der wissenschaftlichen Forschung" for Project 8662 is gratefully acknowledged. H.T. derives partial support from National Science Foundation Grant No. CHE9120158. We also thank Prof. V. N. Sapunov for several useful discussions.

Supplementary Material Available: Listings of anisotropic displacement factors, hydrogen positional and isotropic displacement parameters, complete bond distances and angles, and least-squares planes (26 pages). Ordering information is given on any current masthead page.

(23) (a) Schmidpeter, A.; Lochschmidt, S.; Sheldrick, W. S. *Angew. Chem., Int. Ed. Engl.* **1986**, *25*, 253; (b) Schmidpeter, A.; Lochschmidt, S. *Inorg. Synth.* **1990**, *27*, 253.

(24) Bruce, M. I.; Knight, J. R. *J. Organomet. Chem.* **1968**, 12, 411.
(25) Blum, Y.; Shvo, Y.; Chodosh, D. F. *Inorg. Chim. Acta* **1985**, *97*, L25.
(26) Mays, M. J.; Morris, M. J.; Raithby, P. R.; Shvo, Y.; Czarkie, D. *Organometallics* **1989**, *8*, 1162.